

UCSF

UC San Francisco Previously Published Works

Title

An Evaluation of Robotic and Conventional IMRT for Prostate Cancer: Potential for Dose Escalation

Permalink

<https://escholarship.org/uc/item/094205vs>

Journal

Technology in Cancer Research & Treatment, 16(3)

ISSN

1533-0346

Authors

Pinnaduwage, Dilini S
Descovich, Martina
Lometti, Michael W
et al.

Publication Date


2017-06-01

DOI

10.1177/1533034616639729

Peer reviewed

An Evaluation of Robotic and Conventional IMRT for Prostate Cancer: Potential for Dose Escalation

Technology in Cancer Research & Treatment
2017, Vol. 16(3) 267–275
© The Author(s) 2016
Reprints and permission:
sagepub.com/journalsPermissions.nav
DOI: 10.1177/11533034616639729
journals.sagepub.com/home/tct


Dilini S. Pinnaduwa, PhD¹, Martina Descovich, PhD¹,
Michael W. Lometti, MS¹, Badri Varad, BSc¹, Mack Roach III, MD¹,
and Alexander R. Gottschalk, MD, PhD¹

Abstract

This study compares conventional and robotic intensity modulated radiation therapy (IMRT) plans for prostate boost treatments and provides clinical insight into the strengths and weaknesses of each. The potential for dose escalation with robotic IMRT is further investigated using the “critical volume tolerance” method proposed by Roach et al. Three clinically acceptable treatment plans were generated for 10 prostate boost patients: (1) a robotic IMRT plan using fixed cones, (2) a robotic IMRT plan using the Iris variable aperture collimator, and (3) a conventional linac based IMRT (c-IMRT) plan. Target coverage, critical structure doses, homogeneity, conformity, dose fall-off, and treatment time, were compared across plans. The average bladder and rectum V75 was 17.1%, 20.0%, and 21.4%, and 8.5%, 11.9%, and 14.1% for the Iris, fixed, and c-IMRT plans, respectively. On average the conformity index (nCI) was 1.20, 1.30, and 1.46 for the Iris, fixed, and c-IMRT plans. Differences between the Iris and the c-IMRT plans were statistically significant for the bladder V75 ($P = .016$), rectum V75 ($P = .0013$), and average nCI ($P = .002$). Dose to normal tissue in terms of R50 was 4.30, 5.87, and 8.37 for the Iris, fixed and c-IMRT plans, respectively, with statistically significant differences between the Iris and c-IMRT ($P = .0013$) and the fixed and c-IMRT ($P = .001$) plans. In general, the robotic IMRT plans generated using the Iris were significantly better compared to c-IMRT plans, and showed average dose gains of up to 34% for a critical rectal volume of 5%.

Keywords

robotic IMRT, prostate cancer, dose escalation

Abbreviations

c-IMRT, conventional IMRT; CK, CyberKnife; CT, computed tomography; CVT, critical volume tolerance; DVH, dose–volume histogram; IMRT, intensity-modulated radiation therapy; MLC, multileaf collimator; MU, monitor unit; nCI, new conformity index; PDG, potential dose gain; PIV, prescription isodose volume; PTV, planning target volume; SAD, source-to-axis distance; SED, standard effective dose; VMAT, volumetric-modulated arc therapy

Received: September 09, 2015; Revised: February 11, 2016; Accepted: February 17, 2016.

Introduction

The CyberKnife (CK) robotic radiosurgery system is predominantly used today for stereotactic radiosurgery/body radiotherapy delivery, with typical fractionation schemes ranging

from 1 to 5 fractions. Its application to conventionally fractionated intensity-modulated radiation treatments (IMRTs) has been limited due to the substantially long treatment delivery times and inhomogeneous dose distributions compared to

¹ Department of Radiation Oncology, University of California San Francisco, San Francisco, CA, USA

Corresponding Author:

Dilini S. Pinnaduwa, PhD, Department of Radiation Oncology, University of California San Francisco, 1600 Divisadero Street, Suite H1031, San Francisco, CA 94143, USA.

Email: dilini.pinnaduwa@gmail.com

those on a conventional linear accelerator. However, recent technological developments are increasing the potential of the CK system to be used for robotic IMRT in the clinical setting. The CK-VSI platform introduced a few years ago involves improvements in the delivery efficiency of the system,¹ such as the increased dose rate of a 1000 monitor units (MUs) per minute, 20% increase in the robotic traversal speed, and the availability of the Iris variable aperture collimator. The Iris is composed of 2 banks of 6 tungsten segments each offset by each other to generate dodecahedral apertures. Aperture diameters range from 5 to 60 mm at a source-to-axis distance (SAD) of 800 mm, similar to the aperture diameters available as fixed cones. With the Iris, the robotic linear accelerator traverses the treatment path only once while delivering radiation from multiple collimating apertures. In comparison with the CK fixed cone system, the robot has to traverse the treatment path separately for each fixed cone size used for the treatment. This allows the use of multiple collimating apertures for a treatment, without drastically increasing treatment time. The newly released CK-M6 platform, available for clinical use today, is additionally equipped with a multileaf collimating (MLC) system that provides further potential for improved efficiency in treatment delivery. This MLC system (CK InCise MLC system; Accuray Inc) consists of 41 tungsten leaf pairs of 90 mm height and 2.5 mm thickness at 800 mm SAD and allows for a maximum field size of 120 mm (leaf motion direction) × 100 mm at 800 mm SAD. Leaf motion allows for 100% overtravel and full leaf interdigitation and has an average (intraleaf, interleaf, and leaf tip) transmission of <0.3%.² The VSI and M6 platforms combine continuous image guidance with nonisocentric, noncoplanar treatment delivery with improved efficiency.

The capability to deliver robotic IMRT treatments expands the clinical applications of the CK system. Our motivation to conduct this study was the need to treat prostate patients on the CK to reduce the workload on the other treatment machines, while one linac was being replaced. This brought forth the need to compare the quality of robotic IMRT plans with conventional linac-based IMRT plans.

The purpose of this study is to compare conventional IMRT (c-IMRT) plans with robotic IMRT plans for prostate boost treatments and to provide clinical insight into the strengths and weaknesses of each technique. Further, a “critical volume tolerance” (CVT) analysis is performed to investigate whether robotic IMRT could deliver a higher dose to the prostate without exceeding the normal structure tolerances established for c-IMRT.

Materials and Methods

Ten prostate boost patients treated on the CK-VSI system were chosen for this study. All patients had received c-IMRT to the pelvis (50 Gy in 25 fractions) prior to the prostate boost. For the boost, patients received 2 or 2.5 Gy per fraction, with prescriptions ranging from 17.5 to 28 Gy given in 7 to 14 fractions

Table 1. Prescription and Target Volume Information for Each Case.

Case	Prescription Dose, Gy	No. of Fractions	Dose per Fraction, Gy	PTV, cm ³	Target Area
1	20	10	2	55.66	Prostate bed
2	17.5	7	2.5	30.34	Prostate
3	17.5	7	2.5	60.40	Prostate
4	20	10	2	19.70	Prostate
5	20	10	2	51.86	Prostate bed
6	20	10	2	50.30	Prostate bed
7	28	14	2	79.17	Prostate
8	18	9	2	30.75	Prostate bed
9	20	10	2	28.5	Prostate bed
10	20	10	2	79.27	Prostate bed

Abbreviation: PTV, planning target volume.

(Table 1). The boost treatments were to the localized prostate in 4 of the 10 cases and to the prostate bed in the remaining cases. For the purpose of our study, 3 treatment plans were generated for each patient: (1) a CK plan using fixed collimators, (2) a CK plan using the Iris variable aperture collimator, and (3) a c-IMRT plan.

The same target and critical structure contours were used for generating the 3 plans for each patient. Contours (prostate/prostate bed, planning target volume [PTV], rectum, bladder, bowel, penile bulb) were done on computed tomography (CT) imaging by radiation oncologists specializing in prostate cancer treatment. Prior to CT simulation, all patients had 3 gold markers (1 in the apex and 2 in the base of the prostate) implanted under transrectal ultrasound guidance to be used as surrogates for localizing the prostate during image-guided treatment delivery. In our clinic, treatment plans were generated by a physicist or a dosimetrist who was responsible for generating clinical treatment plans for each modality. Planning dose constraints were based on institutional standards. In general, the rectal and bladder volumes receiving 75%, 50%, and 30% of the prescription dose (denoted as V75, V50, and V30 in this study) were kept below 20%, 50%, and 65% for the composite plan (whole pelvis plus boost treatment). Additionally, the maximum dose within the PTV was kept <120% of the prescription dose, as the urethra is not typically defined for conventional prostate IMRT planning in our clinic.

Robotic IMRT Plan Generation

The robotic IMRT plans were generated in MultiPlan, the CK treatment planning system. For the fixed collimator plans, either 1 or 2 fixed cone sizes were used to limit the treatment time to below 30 minutes. The cone sizes were chosen to optimize both conformality and homogeneity, and, typically, this involved the use of 1 small and 1 large collimator (eg, 15 and 25 mm). For the Iris plans, 6 to 7 apertures ranging from the 12.5 mm aperture to the largest aperture that fits within the PTV were chosen. The number of selected apertures determines the number of nonisocentrically targeted beams that are

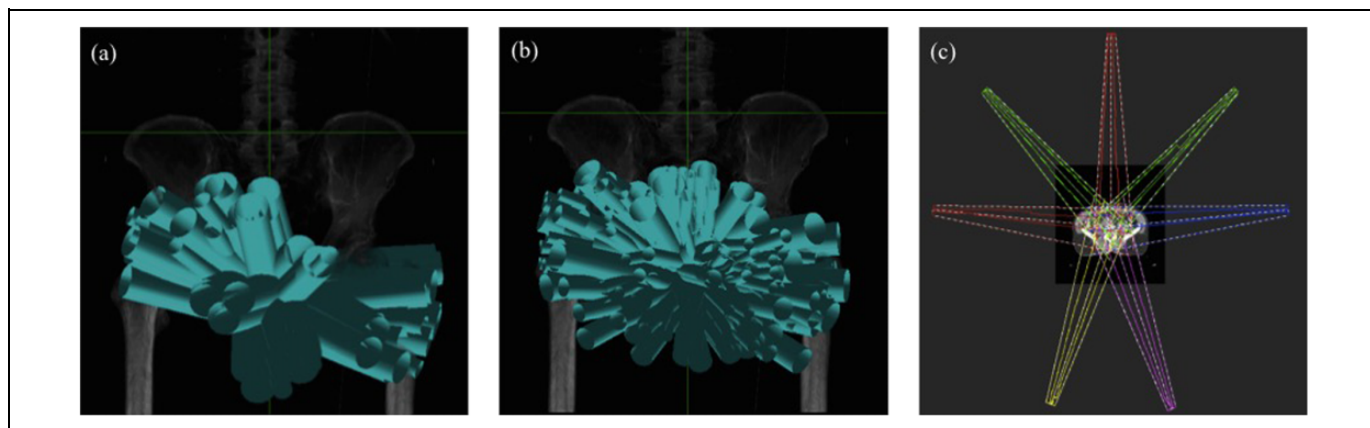


Figure 1. Beam angles for an example single patient (a) robotic IMRT fixed (71 beams), (b) robotic IMRT Iris (178 beams) and (c) conventional IMRT (7 beams) plan.

generated for the optimization, ranging from 1000 beams for a single collimator to 6000 beams for 12 collimators. The CK linear accelerator generates 6-MV photons, with a nominal dose rate of 1000 cGy/min.

The robotic manipulator is programmed to move within a fixed, predetermined workspace. The manipulator and therefore the radiation source can only be positioned at preassigned points within this workspace, referred to as “nodes.” At each node, the linac can deliver radiation from multiple (up to 12) beam angles. Dose is delivered from “paths,” which comprise a series of nodes. The specific nodes for a given treatment are determined during treatment planning, depending on target location and patient anatomy. During treatment delivery, the manipulator moves the accelerator from node to node in sequence and delivers dose at the selected node positions. For this study, we used the “prostate path” or the “reduced prostate path” specifically designed for prostate treatments. The node positions in these 2 paths allow for rotational corrections by the robot up to 2°, 3°, and 5° for the roll, yaw, and pitch rotations, respectively. The reduced prostate path includes a subset of the nodes from the prostate path.

The planning technique for the CK plans was similar regardless of the collimating system. The number of MUs from each node and beam were restricted to below 2000 (range: 800-2000 depending on prescription and fractionation) to allow for a wider distribution (or spread in beam angles) of nonisocentric, noncoplanar beams and to limit a high-dose contribution from a single direction. This helps minimize “dose fingers” (high-dose [typically >40%-50% of the prescription dose] streaks/areas spanning from outside the target volume [TV] toward the skin, which are shaped similar to a finger) and dose hot spots in normal tissue. The maximum MUs per node was set to be slightly higher than the maximum MUs per beam to allow for multiple beams per node. The minimum number of MUs for CK plans was limited to 4 MUs per fraction. To justify this minimum MU cutoff, the linearity of 4 MU beams was measured with respect to 200 MU beams on our CK-VSI system

using the 60-mm cone at a depth of 1.5 cm, and agreement was found to be within 2%.

Shell structures (typically 3-4 shells at varying distances from the target, for example, 0.5-5 mm for the first shell, 5-12 mm for the second shell, and 10-25 mm for the third shell) surrounding the PTV were used as dose tuning structures to achieve a conformal dose distribution around the target and to guide the dose falloff outside the target. In most cases, asymmetric shells (tighter anteriorly and posteriorly compared to the craniocaudal and lateral directions) were used to achieve a tighter dose falloff at the rectum-PTV and bladder-PTV interfaces. Beam entry through the scrotum was prohibited.

Plans were generated using sequential multiobjective optimization³ available in MultiPlan. With this approach, multiple objectives such as target coverage, conformality, homogeneity, and dose-volume limits to organs at risk are optimized in sequence by addressing each objective separately in an order predefined by the user while maintaining user-defined hard constraints (for example, maximum dose within target and maximum doses to the critical structures). Dose was calculated using the ray trace algorithm. Ray trace dose calculation accounts for tissue heterogeneities using a simple effective path length correction algorithm and is appropriate for targets in soft tissue such as the prostate.⁴ Once a plan of acceptable quality is achieved, beam and time reduction tools⁵ were used to obtain a plan that is optimized for treatment efficiency without compromising the dosimetric quality of the plan.

More than a 100 nonisocentric, noncoplanar beams were used in generating the robotic IMRT plans (Figure 1A and B). The average number of nodes, beams, and total MUs used for the Iris and fixed collimator plans, as well as the average of the estimated treatment times as obtained from the treatment planning system, are given in Table 2. The reported times are estimated assuming that the patient is imaged at an imaging interval of 60 seconds during treatment to account for intrafraction prostate motion.

Table 2. Number of Nodes, Beams, Total MUs, and Estimated Treatment Times for the IRIS and Fixed Collimator Robotic IMRT Plans.

	Average No. of Nodes	Average No. of Beams	Total MUs	Treatment Time, minutes
Fixed	35.0 ± 20.0	124.0 ± 26.5	23 138.7 ± 5561.2	25.5 ± 5.9
Iris	59.8 ± 17.0	158.0 ± 47.4	27 177.3 ± 7961.7	27.5 ± 6.0

Abbreviations: IMRT, intensity-modulated radiation therapy; MUs, monitor units.

Conventional IMRT Plan Generation

Conventional IMRT plans were generated per our institutional protocol using Pinnacle (Philips Inc, Cleveland, Ohio). Seven 6-MV beams (anteroposterior, left and right anterior and posterior oblique beams, and 2 near lateral beams) were used for each plan (Figure 1C). The posteroanterior beam was avoided to prevent direct irradiation of the rectum. Instead, the posterior target regions were boosted with posterior oblique beams. Lateral beams were avoided in order to protect the femoral heads. Instead, 2 beams that angle away from the femoral heads, at 85° and 275°, were used. The 2 anterior oblique beams entering at 45° and 315° were chosen so that the beam edges allow for the blocking of the pelvic bones. The minimum segment area was restricted to 4 cm², and the minimum number of MUs per segment was limited to 5. The maximum number of segments allowed was typically set at 50. A 4-cm ring structure surrounding the TV plus a 3-mm margin was used to control dose falloff and the dose to normal tissue surrounding the PTV. Collapsed cone convolution was used for dose calculation.

Conventional IMRT plans were generated for treatment delivery using a Siemens ONCOR (Siemens Healthcare, Erlangen, Germany) linear accelerator. This system utilizes an MLC designed with 41 leaf pairs and consists of 2 pairs of outer leaves that project to a 0.5-cm width and 39 pairs of inner leaves that project to a 1-cm width, at 100 cm from the source.

Robotic IMRT and c-IMRT Plan Comparison

Average dose–volume histograms (DVHs) were generated for plans in each category to compare the doses to the rectum, bladder, TV, and penile bulb. Plans were compared based on target coverage, dose to critical structures (V100, V75, and V50 for the bladder, rectum, and dose to penile bulb), homogeneity, conformity index (new conformity index [nCI]), gradient index, and treatment time. The below definitions of homogeneity⁶ and conformity⁷ indices were used:

$$\text{Homogeneity index} = \frac{\text{the maximum dose normalized by the prescription dose,}}{\text{nCI} = (\text{PIV} \times \text{TV}) / (\text{TIV})^2,}$$

where, PIV is the prescription isodose volume, TV is the target volume, and TIV is the TV inside the prescription isodose.

Dose to normal tissue, in general, was evaluated by looking at the volume enclosed by 50% of the prescription dose

as a ratio to the TV (defined as R50). The average Paddick gradient index used to assess the sharpness of the dose falloff outside the PTV was defined as the volume enclosed by half the prescription isodose normalized to the volume enclosed by the prescription isodose. Paired 2-sample *t* tests were used to determine statistical significance in differences seen between the robotic IMRT Iris and c-IMRT plans, and the robotic IMRT fixed and c-IMRT plans, for the dosimetric parameters investigated. A *P* value of <.05 was used as the threshold in determining statistical significance of the observed differences.

Evaluating the Potential for Dose Escalation With Robotic IMRT Plans

The potential for dose escalation with robotic IMRT compared to c-IMRT was investigated using the CVT method proposed by Roach et al.⁸ This method assumes that a critical threshold dose–volume relationship exists for each type of complication and that exceeding the dose to the critical volume results in unacceptable morbidities or toxicities. It predicts tolerance to radiation for serial structures, assuming that tolerance depends on a critical threshold “low-volume high-dose region.” Two different treatment techniques (eg, a novel technique against a standard technique) can be compared using the CVT method in terms of the potential for safe dose escalation. For example, assume that the threshold dose and the corresponding critical volume of a serial structure that can receive that dose are known based on a standard treatment technique. Then, if a novel treatment technique allows for further sparing of the organ at risk, the potential for dose escalation with that novel technique can be assessed by quantifying the increase in dose to the TV, while maintaining the known critical threshold dose–volume relationship for the organ at risk as per the standard technique.

For our CVT analysis, we looked at the biological effect of the treatments and considered the slightly different fractionation schemes used in our cases using the standard effective dose (SED), as described previously.⁹ The SED expresses the biologically equivalent dose of a fractionation scheme in terms of a standard fraction. For this analysis, we chose the standard fractionation size of 2 Gy. The SED for the critical structure and the prostate for the robotic IMRT plans was defined as:

$$\text{SED}_{\text{PROSTATE}} = \text{ND}_{\text{IRIS}} \frac{(1 + \frac{D_{\text{IRIS}}}{\alpha/\beta})}{(1 + \frac{2.0}{\alpha/\beta})}, \quad (1)$$

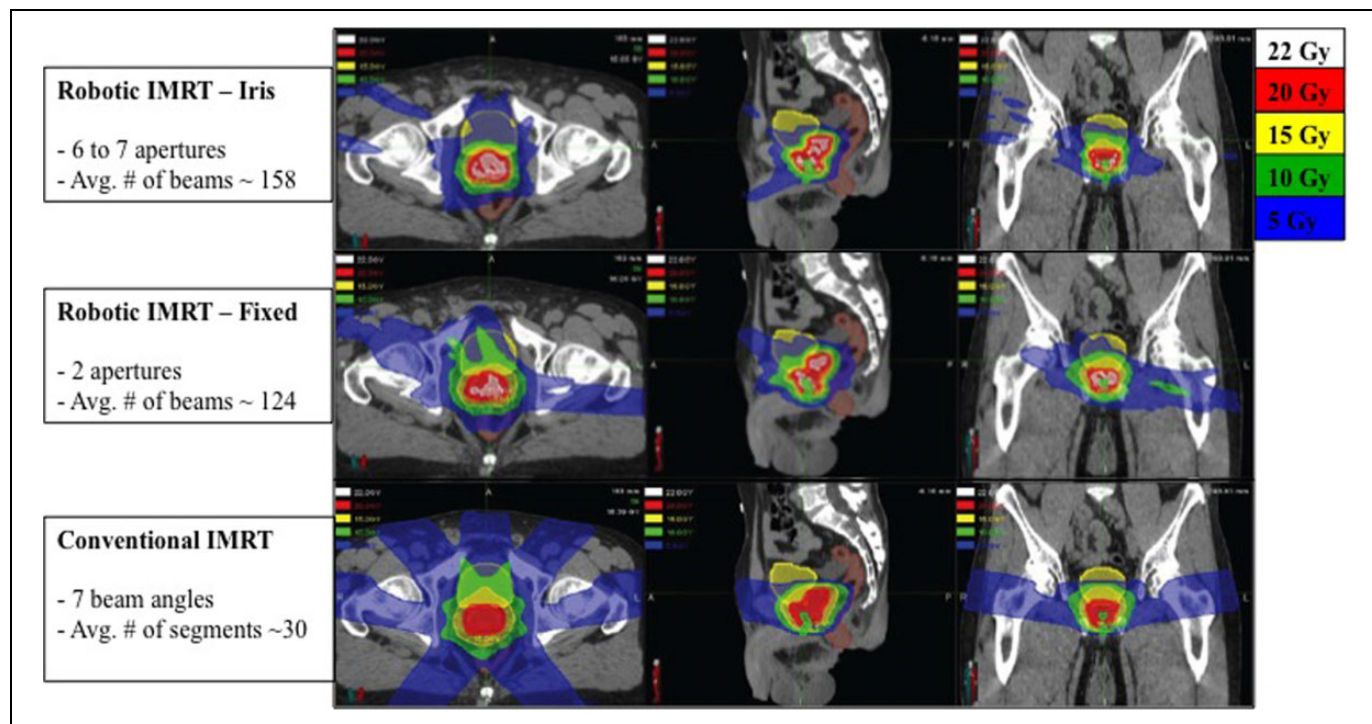


Figure 2. Dose distributions for an example case using the Iris for robotic intensity-modulated radiation therapy (IMRT), fixed cones for robotic IMRT, and conventional IMRT.

$$SED_{CRITICAL} = fND_{IRIS} \frac{(1 + \frac{fD_{IRIS}}{\alpha/\beta})}{(1 + \frac{2.0}{\alpha/\beta})}, \quad (2)$$

where, f is the percentage of the prescribed dose delivered to the critical structure in the robotic IMRT plans, and N is the number of fractions. D_{IRIS} is the maximum dose per fraction that could be delivered with robotic IMRT Iris plans, while maintaining the same $SED_{CRITICAL}$ as that given by the c-IMRT plan.

The $SED_{CRITICAL}$ value is directly read out from the c-IMRT plans for the specific critical volume of tolerance under investigation. Then, the quadratic equation containing $SED_{CRITICAL}$ (Equation 2) is solved to obtain D_{IRIS} . The calculated D_{IRIS} is subsequently used to obtain $SED_{PROSTATE}$ (using Equation 1). The potential dose gain (PDG) is defined as,

$$PDG(\%) = (\frac{SED_{PROSTATE}}{SED_{CRITICAL}} - 1) \times 100.$$

The PDG was calculated based on an α/β of 1.5 and 10 for the prostate and 3.0 for the critical structure.

For our study, we assumed that the rectum was the dose-limiting structure. The PDG for each of the Iris plans was evaluated against the corresponding c-IMRT plan for varying critical volumes of tolerances ranging from 1% to 5% of the rectal volume. The CVT dose was assumed to be the

dose given by the c-IMRT plan to the corresponding critical volume of the rectum.

Results

All plans were clinically acceptable with nearly 95% of the PTV receiving the prescribed dose while meeting dose constraints for the rectum, bladder, and urethra. Example dose distributions of plans from the different treatment delivery techniques are shown in Figure 2.

Dose to the TV

On average, the PTV coverage was 95.7%, 96.3%, and 96.6% for the robotic IMRT-fixed, Iris, and conventional linac IMRT plans, respectively. The average DVHs for the PTV based on the 3 technologies are shown in Figure 3. Differences in the dose heterogeneity within the TV are evident from these average DVHs. The robotic IMRT plans were significantly ($P = .0002$) heterogeneous compared to the conventional linac IMRT plans. The homogeneity index was 1.16 (fixed), 1.16 (Iris), and 1.10 (c-IMRT). The average prescription isodose line was 86.1% for Iris, 85.5% for fixed, and 92.0% for c-IMRT plans.

The robotic IMRT plans were more conformal compared to the conventional IMRT plans, with the plans using the Iris showing the best conformity. The average nCI was 1.20, 1.30, and 1.46 ($P = .002$) for the Iris, fixed, and c-IMRT plans, respectively.

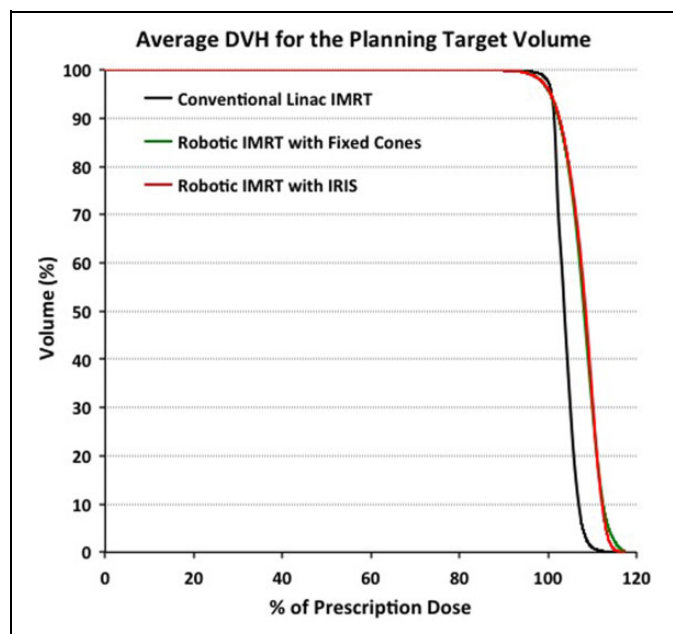


Figure 3. Average dose–volume histograms for planning target volume (PTV), for the conventional linac intensity-modulated radiation therapy (IMRT), and robotic IMRT with fixed and Iris collimators.

Dose to the Rectum and Bladder

The average bladder V75 was 17.1%, 20.3%, and 21.1% and the average rectum V75 was 8.3%, 11.9%, and 14.2% for the Iris, fixed, and IMRT plans, respectively. Robotic IMRT plans resulted in lower V100 and V50 percentages compared to the c-IMRT plans (Table 3). Statistically significant differences were seen between the robotic IMRT plans generated using the Iris and the conventional linac IMRT plans for the rectum V75 ($P = .0014$), V50 ($P = .0002$), and bladder V75 ($P = .016$).

The average DVHs for the rectum (Figure 4A) showed lower rectal doses by 5% to 15 percentage points in the 30% to 90% of the prescription dose range for the Iris plans compared to c-IMRT plans. In comparison, the dose to the rectum was on average lower by 3 to 5 percentage points in the 40% to 90% of the prescription dose range for the robotic IMRT plans using fixed cones compared to c-IMRT. The differences between the bladder DVHs (Figure 4B) were not as prominent. However, the dose to the bladder was lower by 2 to 5 percentage points for the Iris plans in the ~35% to 100% of the prescription dose range compared to c-IMRT. The low dose to the bladder (<40% of the prescription dose) was on average lower for the c-IMRT plans.

Dose to Other Normal Tissue and Dose Falloff

Dose to normal tissue evaluated in terms of R50 was the lowest for the Iris plans, with R50 calculated to be 4.30 for the Iris, 5.87 for the fixed, and 8.37 for the c-IMRT plans. Statistically significant differences in R50 between the Iris and c-IMRT

($P = .0013$) and fixed and c-IMRT ($P = .001$) plans were observed. The average Paddick GI was 3.79, 4.82, and 5.79 for the robotic IMRT Iris, fixed, and c-IMRT plans, respectively, reflecting that the Iris plans had the sharpest dose falloff outside the target.

Prior studies have reported on the association of penile bulb dose with the risk of radiation-induced impotence. A greater risk of impotence has been reported for patients whose median penile bulb dose was ≥ 52.5 Gy compared to those receiving < 52.5 Gy ($P = .039$).¹⁰ In the current study, the average penile bulb dose (Figure 5) was higher for the c-IMRT plans compared to the robotic IMRT plans for nearly up to 50% of the prescription dose. For example, the dose to the penile bulb from c-IMRT was higher by 3 to 5 percentage points in the dose range of ~50% to 90% of the prescription dose and by 0.5 to <3 percentage points in the dose range of 90% to 100% of the prescription dose compared to the Iris plans. These differences seen in the high-dose regions between the different techniques for the radiation boost could be clinically significant when considering the overall composite treatment, since in the whole pelvis c-IMRT portion of some of these cases, the median dose to the penile bulb was already close to the threshold value of 52.5 Gy.

Potential for Dose Escalation With Robotic IMRT Plans

Figure 6A shows the percentage of the prescription dose received by varying percentages of the rectal volume ranging from 2% to 45% for the 3 techniques. Large (nearly ≥ 10 percentage points) differences are seen on average in the dose received by most of the critical volumes considered between the c-IMRT and robotic IMRT plans using the Iris. Differences in the dose received by the critical volumes evaluated were less prominent between the robotic IMRT plans using fixed collimators and the c-IMRT plans.

The average PDGs achievable with robotic IMRT plans using the Iris for varying critical volumes of tolerance is shown in Figure 6B. The PDG ranged from -1.94% to 34.28% (prostate $\alpha/\beta = 1.5$) and -2.24% to 27.70% (prostate $\alpha/\beta = 10$) for the range of CVTs investigated. A negative dose gain implies that the Iris plans do not provide an advantage in terms of dose escalation for that specific critical volume of tolerance under consideration. In other words, at that particular critical volume of tolerance, a higher dose is given to the critical structure by the robotic IMRT Iris plans, compared to what is given by the c-IMRT plans. The dose gain with Iris plans increases as the critical volume of tolerance increases, so if a larger volume of the rectum is capable of tolerating high doses, the potential percentage of dose escalation to the prostate increases.

Discussion

To summarize, looking at the dosimetric differences between the robotic (using the Iris or fixed cones) and the c-IMRT plans for prostate boost patients, dose conformity was the best for the

Table 3. Average Bladder and Rectum Volumes Receiving 100%, 75%, and 50% of the Prescription Dose, Respectively.

	Bladder, %			Rectum, %		
	V ₁₀₀	V ₇₅	V ₅₀	V ₁₀₀	V ₇₅	V ₅₀
Conventional IMRT	9.88	21.37	32.71	2.83	14.14	28.87
Robotic IMRT—fixed cones	8.24	19.96	34.00	2.15	11.95	25.82
(<i>P</i> value, with c-IMRT)	(.517)	(.729)	(.638)	(.225)	(.127)	(.366)
Robotic IMRT—Iris	7.77	17.10	28.70	2.05	8.54	17.78
(<i>P</i> value, with c-IMRT)	(.054)	(.016)	(.207)	(.102)	(.001)	(.0002)

Abbreviations: c-IMRT, conventional IMRT; IMRT, intensity-modulated radiation therapy.

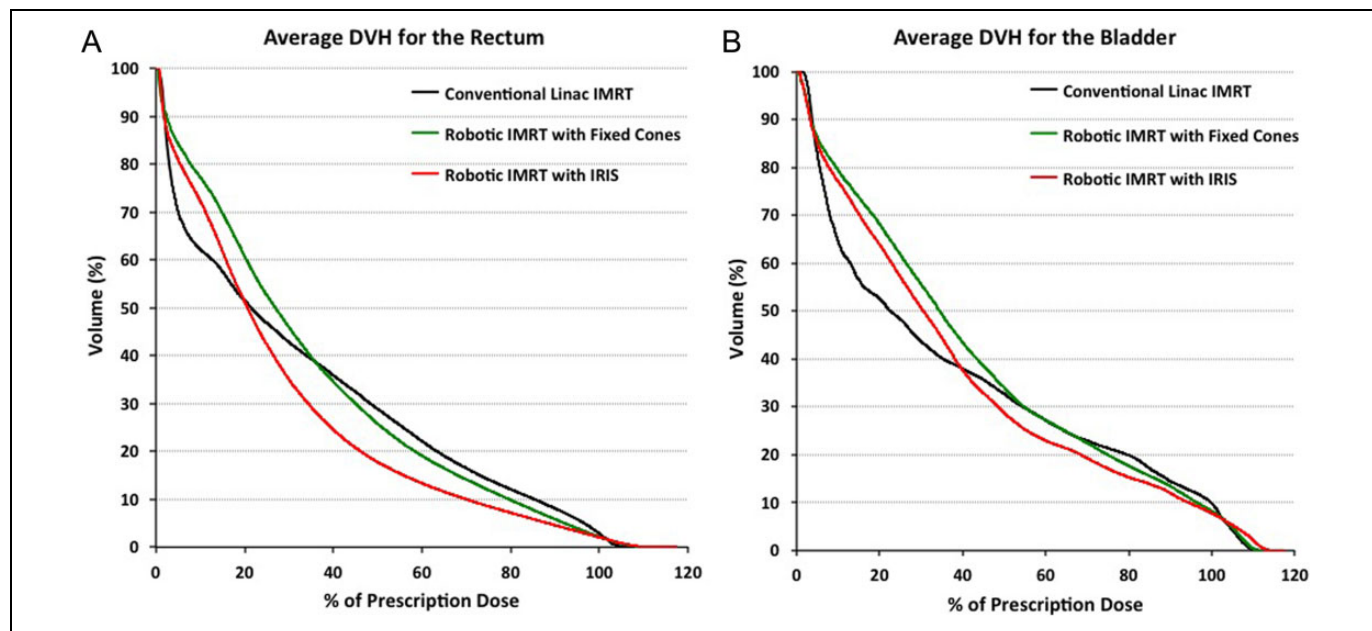


Figure 4. Average dose–volume histograms from the 3 techniques for the (A) rectum and (B) bladder.

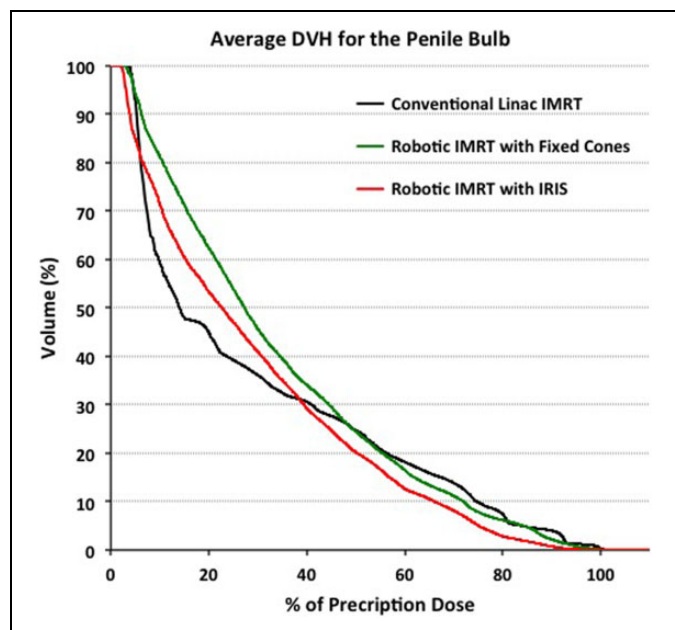


Figure 5. Average dose–volume histogram for the penile bulb, based on plans from the 3 techniques.

Iris plans. When evaluating the dose to the bladder and rectum in terms of the percentage volume receiving 100%, 75%, and 50% of the prescription dose across the 3 techniques, the Iris plans showed the lowest values for all these parameters. Although the bladder percentage volumes receiving 100% and 75% of the prescription dose were lower for the fixed plans compared to the c-IMRT plans, the average bladder V₅₀ was slightly higher (Table 3). This increase in volumes receiving lower dose for the fixed plans compared to the c-IMRT plans (not seen for the Iris plans) is likely a result of having to limit the number of collimators used for planning to 2 fixed cone apertures in order to reduce the treatment time. Further, the Iris plans gave the lowest dose to normal tissue in terms of R₅₀ and showed the sharpest dose falloff. The penile bulb dose was also the lowest for Iris plans in the high-dose regions that may be clinically significant when considering the composite plan doses.

Homogeneity was the highest for the c-IMRT plans. Highly homogenous plans were difficult to achieve with robotic IMRT. This may be due to the CK planners being used to typically generating heterogeneous plans with the CK planning system. We noticed that the homogeneity became an issue when trying to fulfill our requirement of limiting the minimum

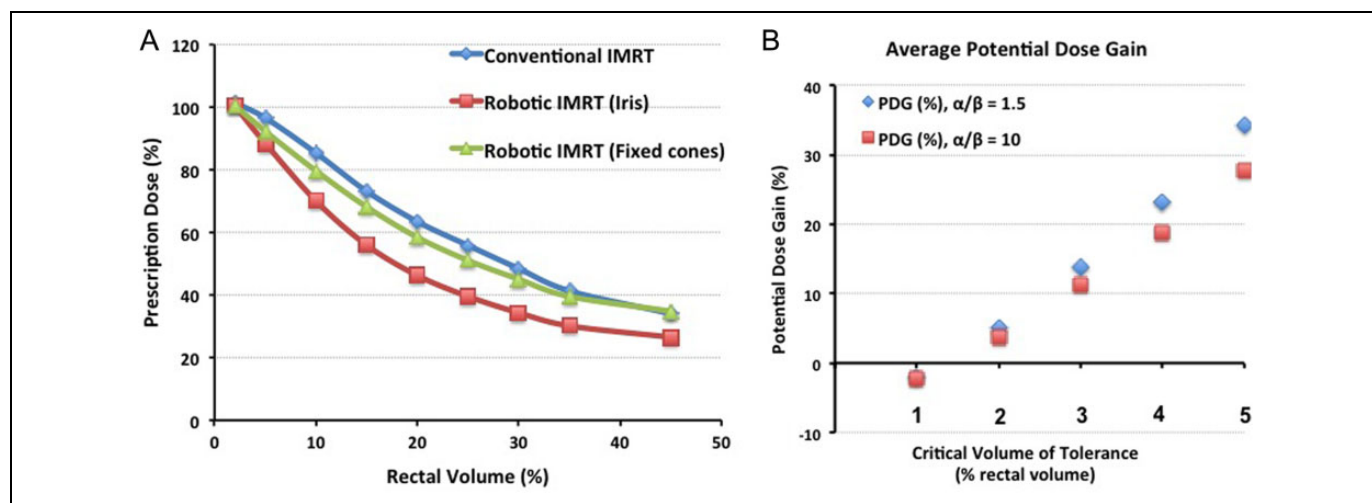


Figure 6. (A) Percentage of the prescription dose received by varying percentages of the rectal volume for the 3 techniques. (B) The potential dose gain with robotic IMRT plans using the Iris compared to conventional IMRT plans for varying critical volumes of tolerance.

number of MUs per beam to be ≥ 4 MUs. Changing the planning technique that was used in our study could help with achieving more homogeneous plans. For example, reducing the number of beam angles or forcing the system to use only large collimators may allow for generating more homogenous CK plans. However, higher homogeneity will likely be achieved at the expense of having to compromise the high conformality and sharper dose falloff seen with robotic IMRT.

Another option would be to define the urethra for these cases using either MRI or a contrast CT and to limit the dose to the urethra during the inverse optimization process. This would eliminate the homogeneity requirement of prescribing to the 85% isodose or higher. Eliminating the homogeneity requirement would allow us to achieve plans with steeper dose gradients and further spare the rectum and bladder, thus potentially allowing for dose escalation. Additionally, with the CK system, we are able track and correct for prostate motion during treatment delivery. This reduces the uncertainty in target localization during treatment. Therefore, robotic IMRT provides the potential for reducing the PTVs¹¹ compared to those used for c-IMRT. Previous investigators¹² have evaluated PTV margins as a function of imaging frequency in prostate robotic radiotherapy and found that a 2-mm margin is required for a 60-second imaging time interval.

However, while dosimetrically the robotic IMRT plans were better and may provide an avenue for further dose escalation, the estimated treatment times were nearly 2 times longer compared to c-IMRT treatments. In general, a larger (5-7 times higher) number of MUs were used in robotic IMRT plans compared to c-IMRT plans, resulting in a higher integral dose to the patient. However, this is likely not a major concern for patients with prostate cancer.

In this study, we used a 7-field step-and-shoot technique for generating our c-IMRT plans. This was our institutional standard at the time of data acquisition for the dosimetric

comparison carried out here. Although clinics are currently moving toward using more advanced techniques such as volumetric-modulated arc therapy (VMAT), a recent study¹³ comparing variable dose-rate VMAT with 7-field step-and-shoot IMRT for prostate cancer saw no significant difference between the groups in terms of rectal V_{60} , V_{65} , V_{70} , V_{75} and bladder V_{65} , V_{70} , V_{75} , V_{80} . However, VMAT resulted in shorter beam-on times and more homogenous dose distributions.

Although achieving highly homogeneous plans were difficult with the CK-VSI system, McGuinness et al¹⁴ have shown that the CK-MLC system in the M6 platform is capable of generating highly homogeneous plans similar to those achievable with conventional linear accelerators and that the CK-MLC system provides significant improvements in terms of homogeneity and treatment time compared to the CK systems with circular collimators. Therefore, these new CK systems equipped with the MLC hold promise for faster and more efficient delivery of IMRT plans.

Conclusion

Dosimetrically, robotic IMRT plans using the Iris provided better sparing of critical structures compared to c-IMRT plans in our investigation. Thus, robotic IMRT potentially provides an avenue for dose escalation while conforming to tolerance dose constraints for the critical structures.

Declaration of Conflicting Interests

The author(s) declared no potential conflicts of interest with respect to the research, authorship, and/or publication of this article.

Funding

The author(s) received no financial support for the research, authorship, and/or publication of this article.

References

1. Kilby W, Dooley JR, Kuduvalli G, et al. The CybrKnife® robotic radiosurgery system in 2010. *Technol Cancer Res Treat*. 2010; 9(6):433-452.
2. Accuray Inc. *CyberKnife M6 Series Technical Specifications*. Madison, WI: Accuray; 2013.
3. Schlaefler A, Schweikard A. Stepwise multi-criteria optimization for robotic radiosurgery. *Med Phys*. 2008;35(5):2094-2103.
4. Wilcox E, Daskalov GM, Lincoln H. Stereotactic radiosurgery-radiotherapy: should Monte Carlo treatment planning be used for all sites? *Pract Radiat Oncol*. 2011;1(4):251-260.
5. Kilby W, Dooley JR, Kuduvalli G, Sayeh S, Maurer CR Jr. The CyberKnife robotic radiosurgery system in 2010. *Technol Cancer Res Treat*. 2010;9(5):433-452.
6. Paddick IA. A simple scoring ratio to index the conformity of radiosurgical treatment plans. Technical note. *J Neurosurgery*. 2000;93(suppl 3):219-222.
7. Nakamura JL, Varhey LJ, Smith V, et al. Dose conformity of gamma knife radiosurgery and risk factors for complications. *Int J Radiat Oncol Biol Phys*. 2001;51(5):1313-1319.
8. Roach M III, Pickett B, Weil M, Verhey L. The "critical volume tolerance method" for estimating the limits of dose escalation during three-dimensional conformal radiotherapy for prostate cancer. *Int J Rad Oncol Biol Phys*. 1996;35(5):1019-1025.
9. Hsu IC1, Pickett B, Shinohara K, Krieg R, Roach M III, Phillips T. Normal tissue dosimetric comparison between HDR prostate implant boost and conformal external beam radiotherapy boost: potential for dose escalation. *Int J Rad Oncol Biol Phys*. 2000; 46(4):851-858.
10. Roach M III, Winter K, Michalski J, et al. Penile bulb dose and impotence after three-dimensional conformal radiotherapy for prostate cancer on RTOG 9406: Findings from a prospective, multi-institutional, phase I/II dose-escalation study. *Int J Rad Oncol Biol Phys*. 2004;60(5):1351-1356.
11. Gottschalk AR, Hossain S, Chuang C, et al. Intrafraction prostate motion during CyberKnife radiosurgery: implications on planning margins [abstract]. *Int J Rad Oncol Biol Phys*. 2008;72(1):s569.
12. Xie Y, Djajaputra D, King CR, Hossain S, Ma L, Xing L. Intrafractional motion of the prostate during hypofractionated radiotherapy. *Int J Radiat Oncol Biol Phys*. 2008;72(1):236-246.
13. Mellon EA, Javedan K, Strom TJ, et al. A dosimetric comparison of volumetric modulated arc therapy with step-and-shoot intensity modulated radiation therapy for prostate cancer. *Pract Radiat Oncol*. 2015;5(1):11-15.
14. McGuinness CM, Gottschalk AR, Lessard E, et al. Investigating the clinical advantages of a robotic linac equipped with a multi-leaf collimator in the treatment of brain and prostate cancer patients. *J Appl Clin Med Phys*. 2015;16(5):5502.